

1 Neutron production in terrestrial gamma-ray flashes

B.E. Carlson,¹ N. G. Lehtinen,¹ and U.S. Inan^{1,2}

B. E. Carlson, STAR Lab, Electrical Engineering Department, Stanford University, 350 Serra Mall, Packard Bldg., Stanford, CA 94305-9515

N. G. Lehtinen, STAR Lab, Electrical Engineering Department, Stanford University, 350 Serra Mall, Packard Bldg., Stanford, CA 94305-9515

U. S. Inan, Koç University, Rumelifeneri Yolu, 34450 Sariyer, Istanbul, Turkey

¹Space, Telecommunications and Radioscience Laboratory, Electrical Engineering Department, Stanford University, Stanford, California, USA

²Koç University, Sariyer, Istanbul, Turkey

2 **Abstract.** Terrestrial gamma-ray flashes are brief bursts of photons with
3 energies up to 20 MeV typically observed in association with lightning. Such
4 energetic photons may undergo photonuclear reactions with nontrivial cross
5 section in the vicinity of the giant dipole resonance. Pulses of neutrons have
6 been observed experimentally in coincidence with lightning, suggesting such
7 reactions are observable. We present simulations of expected photoneutron
8 production based on initial conditions inferred from observations of TGFs.
9 We predict an average of $\sim 10^{12}$ neutrons produced per TGF and give en-
10 ergy, time, and space distributions of neutrons produced and neutrons reach-
11 ing ground and satellite altitude. The simulation results are consistent with
12 some observations and suggest further experiments may be profitable.

1. Introduction

13 Terrestrial gamma-ray flashes (TGFs) are intense pulses of energetic photons observed
14 by satellites with a fluence of ~ 1 photon/cm², a timescale of ~ 0.5 ms and photon energies
15 of up to 20 MeV when seen from orbit [*Fishman et al.*, 1994; *Smith et al.*, 2005; *Grefen-*
16 *stette et al.*, 2009; *Grefenstette et al.*, 2008]. TGFs are typically observed in close time
17 coincidence with detectable lightning discharge within 300 km of the subsatellite point
18 [*Inan et al.*, 2006; *Cohen et al.*, 2006; *Cummer et al.*, 2005; *Stanley et al.*, 2006]. Though
19 the details of the production mechanism are the subject of much discussion with many
20 mechanisms proposed, [see *Inan and Lehtinen*, 2005; *Lehtinen et al.*, 1996; *Milikh and Val-*
21 *divia*, 1999; *Fargion*, 2002; *Paiva et al.*, 2009; *Milikh et al.*, 2005; *Dwyer*, 2008; *Carlson*
22 *et al.*, 2009], the rough properties of TGFs are known. In particular the very hard average
23 spectrum of observed TGF photons requires a bremsstrahlung photon source altitude of
24 15–20 km [*Dwyer and Smith*, 2005; *Carlson et al.*, 2007]. Assuming the photons are uni-
25 formly distributed over a disk of radius 300 km (given by the typical lightning-subsatellite
26 distance), the 1 photon/cm² fluence implies that of order 10^{15} photons reach satellite al-
27 titude. Full comparison of satellite observations to simulations of photon attenuation
28 and scattering in the atmosphere requires a source of photons with 15–20 km altitude,
29 uniform photon directional distribution with zenith angle $\theta < 45^\circ$, and a total source of
30 4×10^{15} – 4×10^{16} photons on average, with broader beams requiring source populations
31 as high as 10^{17} photons [*Carlson et al.*, 2007].

32 This large number of photons with an energy spectrum extending up to and above
33 20 MeV suggests that photonuclear reactions should occur. For example, the dominant

34 process for nitrogen, photoneutron production, $^{14}\text{N}(\gamma, n)^{13}\text{N}$, occurs for photons with
35 energies $\mathcal{E}_\gamma > 10.55\text{ MeV}$ with an energy-dependent cross section exhibiting a large peak
36 at $\sim 23\text{ MeV}$, the so-called giant dipole resonance [*Chadwick et al.*, 2000; *Berman and*
37 *Fultz*, 1975]. For nitrogen, the peak cross section is ~ 14 millibarns. For comparison, the
38 pair production and Compton scattering cross sections for photons in this energy range
39 are roughly equal and are approximately 170 millibarns [*Cullen et al.*, 1997]. Photonuclear
40 processes therefore amount to a maximum of about 5% of the total photon interaction
41 cross section. This implies Compton scattering and pair production are dominant and
42 that neutron production does not significantly affect energetic photon behavior. Energetic
43 neutrons, however, if they are produced in large enough quantities, are interesting as they
44 are highly penetrating and are not easily attenuated. For context, the mean free path for
45 energetic photons at sea level is of order 1 km (pair production and Compton scattering
46 dominate), while the mean free path for energetic neutrons is of order 0.3 km (elastic
47 scattering dominates). TGFs should therefore be accompanied by neutron production.

48 This idea has been suggested previously in work by Leonid Babich and others. Specifi-
49 cally, *Babich* [2006] raises the possibility of photonuclear reactions associated with TGFs
50 in the context of the upward atmospheric discharge model described in *Babich et al.* [2004].
51 *Babich et al.* [2007] and *Babich et al.* [2008] further develop this idea, and *Babich and*
52 *Roussel-Dupré* [2007] describes the relation of these analyses to the existing experiments
53 discussed below. Overall, these works indicate that the upward atmospheric discharge
54 model produces $\sim 10^{15}$ neutrons, but the properties of these neutrons are not specified
55 and the results of the upward atmospheric discharge model may be questionable in the

56 context of TGFs given the extremely poor spectral fits seen in Figure 5 of *Babich et al.*
57 [2008].

58 Neutron bursts have been reported in conjunction with lightning indicating $10^9 - 10^{10}$
59 neutrons are produced per lightning discharge [*Shah et al.*, 1985; *Shyam and Kaushik*,
60 1999]. Neutron count rates observed from orbit show occasional excess count rates in equa-
61 torial regions suggested to be caused by neutron production by lightning [*Bratolyubova-*
62 *Tsulukidze et al.*, 2004]. Whether neutrons observed in conjunction with lightning are
63 produced by photonuclear processes in a TGF-like event is uncertain. Fusion processes
64 have also been suggested as relevant [*Libby and Lukens*, 1973], but more detailed analysis
65 indicates photonuclear processes are more likely [*Babich*, 2006].

66 In this paper, we use the inferred source spectrum of terrestrial gamma-ray flashes to
67 drive Monte Carlo simulations of photoneutron production. The simulation results are
68 used to predict the properties of the neutrons produced and the properties of neutrons that
69 may be observable. Our results indicate that TGF production at 15–20 km altitude should
70 be accompanied by production of 3×10^{11} – 3×10^{12} neutrons. This is fewer than the pre-
71 dictions of 10^{15} neutrons produced by Babich’s upward atmospheric discharge model, but
72 is more than that suggested to be produced in conjunction with lightning. We additionally
73 give the energy, arrival time, and position distributions of neutrons as produced and at
74 ground and satellite altitudes. Our results are consistent with the ground observations of
75 lightning-associated neutron pulses in *Shah et al.* [1985] and *Shyam and Kaushik* [1999]
76 but are not consistent with satellite observations of *Bratolyubova-Tsulukidze et al.* [2004].

2. Simulation of Neutron production by TGFs

We predict neutron production by Monte Carlo simulations of photonuclear reactions caused by TGF photons. We use the GEANT4 software package [Agostinelli *et al.*, 2003], a high-energy physics Monte Carlo simulation tool that includes all relevant electromagnetic and nuclear physics including Compton scattering, pair production, photoneutron production, neutron elastic and inelastic scatter, and radiative capture. Photonuclear reactions for nitrogen, oxygen, and argon, in particular, are approximated in the giant dipole resonance regime with a parametrization and interpolation scheme involving data from ^{12}C , ^{16}O , ^{27}Al and ^{40}Ca . Comparison of the cross section used in GEANT4 to measured cross sections shows that this scheme matches the cross section to better than a factor of 2, with systematic underestimate of the cross section just above the minimum energy threshold [Kossov, 2002].

The initial conditions for these simulations are chosen to match our knowledge of TGFs and to cover reasonable scenarios for neutron emission. First consider a population of electrons with energy distribution characteristic of electric-field-driven avalanche growth of populations of relativistic particles as described in Lehtinen *et al.* [1999]. The bremsstrahlung spectrum produced by these electrons does not depend strongly on the strength of the electric field or the altitude of the electric field region, provided the electric field exceeds the runaway relativistic electron avalanche threshold [Dwyer and Smith, 2005]. We start our simulation with photons drawn from this spectrum, ignoring photons with energies below the lowest relevant photoneutron production threshold (9.87 MeV for argon). Only approximately 1% of the original TGF source photons exceed this cutoff energy. While there are undoubtedly spectral differences between TGFs, this initial pho-

99 ton spectrum matches the observed average TGF spectrum very well for source altitudes
100 15–20 km [*Carlson et al.*, 2007] and thus provides a good measure of the average TGF
101 initial photon spectrum.

102 These initial photons are placed in point sources at 2.5, 5, 7.5, 10, 15, and 20 km al-
103 titudes, spanning the allowed range of altitudes for TGF production and extending to
104 lower altitudes to explore possible ground observations. Such point sources are useful as
105 they produce the most compact source of neutrons and can be superposed to construct
106 larger distributed sources. The atmospheric density profile is taken from *Hedin* [1991].
107 At each altitude, the initial photon directions are either distributed isotropically or are
108 distributed uniformly over a cone with half-opening angle 20° directed either upwards or
109 downwards. Photons may be emitted isotropically by electrons driven by nontrivial elec-
110 tric field structure, while 20° beams are characteristic of bremsstrahlung from runaway
111 relativistic electron avalanches driven by uniform electric fields. The behavior of these
112 initial photons is then simulated with GEANT4. Every neutron produced in the simula-
113 tion is tracked and neutrons that travel below 0.5 km altitude (ground) or above 350 km
114 altitude (representing escape to satellite altitude) are recorded. One million initial pho-
115 tons are simulated for each set of initial conditions. The numbers of neutrons produced
116 and recorded in these simulations are given in Table 1.

117 As discussed previously, 4×10^{15} – 4×10^{16} energetic photons are produced in an average
118 TGF as observed by RHESSI [*Carlson et al.*, 2007]. Of these source photons, an average
119 of $\sim 1\%$ or $\sim 10^{14}$ exceed the threshold for photonuclear reactions. The numbers in
120 Table 1 give approximately 6400 neutrons produced per million photons with energy
121 above the photonuclear reaction cutoff, giving 3×10^{11} – 3×10^{12} neutrons produced in an

122 average TGF. This is roughly two orders of magnitude lower than the 10^{14} – 10^{15} previously
123 predicted [*Babich et al.*, 2008; *Babich et al.*, 2007; *Babich*, 2006], a fact we return to below
124 in the Discussion.

125 In the initial simulations no neutrons were recorded for certain conditions, for example
126 neutrons that reach ground for upward-directed initial photons at 20 km. This does not
127 mean neutron observation under such conditions is impossible, only that it is not resolved
128 in our initial simulations. To improve the statistics, we run a second round of simulations,
129 starting not with energetic photons, but with energetic neutrons as produced in our first
130 round of simulations. This improves the statistics of neutron propagation but does not
131 improve the statistics of neutron production. The improved estimates of the number of
132 neutrons matching the given conditions from this second round of simulations are given
133 in parentheses in Table 1.

134 As the initial photon energy distribution is constant and photon-neutron production takes
135 place almost entirely with unscattered photons, the produced neutron energy distribution
136 is roughly constant and is shown as the solid black line in Figure 1. The mean produced
137 neutron energy is 3.9 MeV (median 3.6 MeV). Figure 1 also shows sample energy spectra
138 of neutrons reaching ground and satellite levels (black dotted and grey solid lines, re-
139 spectively). Such neutrons have been partially thermalized after propagation through the
140 atmosphere and have a mean energy of 2.0 MeV (median 1.3 MeV) with a substantially
141 shifted distribution.

142 Sample distributions of neutron production positions are shown in Figure 2. The neu-
143 trons are often produced far from the initial photon source, consistent with the energetic

144 photon mean free path of $\sim 1 \text{ km} \times \exp(z/H)$ where z is the altitude and H is the atmo-
145 spheric scale height ($H \sim 8 \text{ km}$).

146 The arrival time distributions for neutrons at ground and satellite altitudes from instan-
147 taneous photon point sources are shown in Figure 3. Neutrons arriving at ground level
148 from point photon sources at 2.5 km and 5 km are shown in the left panel, while the time
149 distribution for neutrons arriving at satellite altitudes from 15 km and 20 km are shown
150 in the right panel. Ground level neutrons from an instantaneous photon source arrive
151 in a pulse $\sim 10 \mu\text{s}$ long with a pronounced tail, a time short compared to a typical TGF
152 timescale of 0.5 ms. Neutrons arriving at satellite altitude are substantially more dispersed
153 due to their longer path lengths, and arrive spread over a pulse $\sim 50 \text{ ms}$ long, much longer
154 than a typical TGF timescale. Consequently, ground-level neutron arrival times should
155 reflect the timescale of their production, while arrival times at satellite altitude are widely
156 spread due to longer path lengths. Note also that the ground-level neutron detections in
157 *Shah et al.* [1985] show neutron arrival up to 10–100 ms after the trigger time, much longer
158 than the typical arrival time delay shown in Figure 3. This delay suggests a source not
159 intimately connected with the triggering electromagnetic signal. Such a time delay may
160 be due to activity elsewhere in the discharge not directly associated with the process that
161 resulted in the trigger.

162 We also give results of simulations of isotropic point sources of neutrons drawn from
163 the characteristic energy spectrum shown in Figure 1. Expected numbers of neutrons
164 are shown in Table 2. These results are not representative of the distributed sources of
165 neutrons shown in Figure 2, but are useful for understanding of photoneutron propaga-
166 tion in the atmosphere. In particular, a simple treatment of exponential attenuation and

167 r^{-2} decrease underestimates the flux by a factor of 6 for the first row in Table 2, with
168 progressively worse error as altitude increases. Proper correction of this error by account-
169 ing for scattering effectively requires table lookup of accumulation factors, precisely the
170 information provided in Table 2.

171 Sample radial distributions of the flux of neutrons arriving at ground and satellite
172 altitudes from point sources at various altitudes are shown in Figure 4. Neutrons at
173 ground level cover a disk roughly 1 km in radius, while longer path lengths lead to a much
174 broader ~ 400 km radius disk at 350 km altitude. At ground level, higher source altitudes
175 result in slightly broader neutron distribution, but the bulk of the neutrons still arrive
176 less than 1 km from the sub-source point if the source is less than 3 km from the ground.

3. Discussion

177 On the basis of TGF observations and the resulting constraints on the source described
178 in *Carlson et al.* [2007], we estimate $\sim 10^{12}$ neutrons produced per TGF on average. This
179 is a factor of ~ 100 smaller than existing predictions derived from a discharge model
180 [*Babich et al.*, 2008; *Babich et al.*, 2007; *Babich*, 2006]. The discrepancy is likely due
181 to different initial photon population sizes and different photon spectra. The discharge
182 model of [*Babich*, 2006] predicts the TGF source photon population size to be 10^{17} with
183 a spectrum capable of producing 10^{15} neutrons [*Babich and Roussel-Dupré*, 2007], while
184 the results described above together with those of *Carlson et al.* [2007] show that the
185 RHESSI and BATSE TGF data require a source of $\sim 10^{16}$ photons with a spectrum
186 shown here to be only capable of producing 10^{12} neutrons. Energetic processes lower
187 in the atmosphere not associated with TGFs such as the gamma-ray burst observed at
188 ground level in association with triggered lightning described in *Dwyer et al.* [2004] may

189 of course have different characteristics and correspondingly higher or lower photon and
190 neutron yields. *Babich and Roussel-Dupré* [2007], for instance, estimates the photon
191 yield for the *Dwyer et al.* [2004] event to be 3×10^{19} , though this is almost certainly an
192 overestimate, with the resulting neutron yields given as 4×10^{13} .

193 Assuming our estimate of $\sim 10^{12}$ neutrons produced in an average TGF, the number of
194 neutrons arriving at ground level from a downward-directed photon source at 5 km can be
195 calculated from the numbers in Table 1 as $\sim 1 \times 10^9$. These neutrons, spread over a disk
196 1 km in radius give an average fluence of $3 \times 10^{-2} \text{ cm}^{-2}$. A similar source at 2.5 km gives
197 an average fluence of 1 cm^{-2} . These fluxes are grossly consistent with the observations
198 in *Shah et al.* [1985] which see pulses of more than one neutron with an effective area of
199 $3 \times 10^4 \text{ cm}^2$ in temporal coincidence with lightning. Similar results were also observed in
200 *Shyam and Kaushik* [1999], but they do not give the effective area of their detector so a
201 full comparison is not possible. Both *Shyam and Kaushik* [1999] and *Shah et al.* [1985]
202 assume the neutrons were produced locally by a lightning discharge and thus estimate
203 lower numbers of neutrons produced. Our results here suggest that their results may also
204 be explained by more distant neutron sources due to photonuclear processes. Note that
205 as energetic photons have a longer mean free path than neutrons, photoproduction of
206 neutrons implies that neutron observations should be accompanied by energetic photon
207 observations.

208 Neutrons that escape to 350 km altitude are spread over a region roughly 400 km in
209 radius, giving a fluence of 10^{-5} cm^{-2} for the upward-directed photon source at 15 km con-
210 sistent with satellite observations of TGFs. Though the number of neutrons that escape
211 to satellite altitude from high-altitude photon sources are greater than the numbers that

212 reach ground level from low-altitude sources, the greater area covered by the emissions
213 drastically reduces the flux. *Bratolyubova-Tsulukidze et al.* [2004] examined data from
214 neutron detectors on satellites of effective area 30 cm^2 and 100 cm^2 . With these effective
215 areas, our results indicate that individual neutron bursts of the sort suggested here on the
216 basis of TGF observations would be undetectable by the instruments analyzed. Statisti-
217 cally, optimistically assuming that every lightning discharge produces a TGF-like energetic
218 photon burst and that every lightning discharge happens within 400 km of the satellite,
219 the global lightning frequency of 40 Hz would give the count rate due to lightning-induced
220 photonuclear processes as 4×10^{-2} Hz. As even this extremely optimistic estimate is be-
221 low the lowest background count rate observed in *Bratolyubova-Tsulukidze et al.* [2004]
222 of ~ 0.5 Hz, our results indicate that the observations in *Bratolyubova-Tsulukidze et al.*
223 [2004] are not due to photonuclear reactions in TGF-like processes.

224 Photoneutrons produced by energetic photons in a TGF-like event should therefore be
225 observable at ground level if the photon source has ≤ 5 km altitude. Our predictions are
226 consistent with existing observations of neutron bursts associated with lightning. This
227 suggests that these observations may be explained by photonuclear interactions of high-
228 energy photons produced in a TGF-like process. The presence of photoneutrons indicates
229 the presence of ≥ 10 MeV photons, a strong proxy for the presence of energetic electrons
230 and runaway relativistic electron avalanche, a process suggested as relevant to many as-
231 pects of thunderstorm and atmospheric physics including lightning initiation [e.g. *Dwyer,*
232 *2005; Marshall et al., 2005; Gurevich et al., 1999*], high-frequency radio emissions [e.g.
233 *Tierney et al., 2005*], and sprite and blue jet formation [e.g. *Lehtinen et al., 1999; Babich*
234 *et al., 2007; Roussel-Dupré and Gurevich, 1996*]. Further searches for these neutrons, in-

cluding more detailed studies of their time and space distribution in relation to causative lightning, should therefore help shed light on these topics.

4. Summary

We give the results of simulations of photoneutron production as motivated by TGF observations. Our results indicate that $\sim 10^{12}$ energetic neutrons are produced per TGF with distributions in energy, space and time as shown in the figures. The fractional production of photoneutrons and the fraction that reach ground level or escape to satellite altitude are given in Tables 1 and 2. If the photon source is at a sufficiently low altitude, these neutrons will be observable on the ground with temporal and radial distributions given in Figures 3 and 4. The properties of the emissions predicted are consistent with ground observations of neutrons coincident with lightning discharge. Further observations of neutrons are necessary to clarify the connections between lightning, TGFs, neutrons, and other energetic atmospheric phenomena. In particular, measurements of the time and space distributions of lightning-associated neutron emissions could be compared to our results here and used to infer the properties of the neutron source. Such analysis would help answer such open questions as whether or not all lightning produces energetic photons, whether or not all lightning produces energetic neutrons, and if coincidences between lightning and neutron measurements are always accompanied by energetic photons.

Acknowledgments. The authors wish to thank Martin Walt for very useful discussions. This work was supported by the National Science Foundation under grant ATM-0535461.

References

- 255 Agostinelli, S., et al. (2003), G4—a simulation toolkit, *Nucl. Inst. & Meth.*, 506(3), 250–
256 303.
- 257 Babich, L. P. (2006), Generation of neutrons in giant upward atmospheric discharges, *Sov.*
258 *Phys.–JETP*, 84, 285–288, doi:10.1134/S0021364006180020.
- 259 Babich, L. P., and R. A. Roussel-Dupré (2007), Origin of neutron flux increases ob-
260 served in correlation with lightning, *J. Geophys. Res.*, 112(D11), 13,303, doi:10.1029/
261 2006JD008340.
- 262 Babich, L. P., R. I. Il’kaev, I. M. Kutsyk, K. I. Bakhov, and R. A. Roussel-Dupré (2004),
263 Self-consistent calculation of upward atmospheric discharge developing in the mode
264 relativistic runaway electron avalanches, *Geomag. Aeron.*, 44(2), 231–242.
- 265 Babich, L. P., K. A. Yu., K. M. L., and K. I. M. (2007), Terrestrial gamma-ray flashes
266 and neutron pulses from direct simulation of gigantic upward atmospheric discharge,
267 *Sov. Phys.–JETP Lett.*, 85(10), 483–487, doi:10.1134/S0021364007100037.
- 268 Babich, L. P., A. Y. Kudryavtsev, M. L. Kudryavtseva, and I. M. Kutsyk (2008),
269 Atmospheric gamma-ray and neutron flashes, *Sov. Phys.–JETP*, 106, 65–76, doi:
270 10.1007/s11447-008-1005-4.
- 271 Berman, B. L., and S. C. Fultz (1975), Measurements of the giant dipole resonance with
272 monoenergetic photons, *Rev. Mod. Phys.*, 47, 713–761, doi:10.1103/RevModPhys.47.
273 713.
- 274 Bratolyubova-Tsulukidze, L., E. Grachev, O. Grigoryan, V. Kunitsyn, B. Kuzhevskij,
275 D. Lysakov, O. Nechaev, and M. Usanova (2004), Thunderstorms as the probable reason
276 of high background neutron fluxes at $L < 1.2$, *Adv. Space Res.*, 34(8), 1815–1818.

- 277 Carlson, B. E., N. G. Lehtinen, and U. S. Inan (2007), Constraints on terrestrial gamma
278 ray flash production from satellite observation, *Geophys. Res. Lett.*, *34*, L08,809, doi:
279 10.1029/2006GL029229.
- 280 Carlson, B. E., N. G. Lehtinen, and U. S. Inan (2009), Terrestrial Gamma-ray Flash
281 Production by Lightning Current Pulses, *J. Geophys. Res.*, doi:10.1029/2009JA014531,
282 in press.
- 283 Chadwick, M., et al. (2000), Handbook of photonuclear data for applications: Cross
284 sections and spectra, *IAEA TECH-DOC*, *1178*.
- 285 Cohen, M. B., U. S. Inan, and G. Fishman (2006), Terrestrial gamma ray flashes ob-
286 served aboard the Compton Gamma Ray Observatory/Burst and Transient Source
287 Experiment and ELF/VLF radio atmospherics, *J. Geophys. Res.*, *111*, D24,109, doi:
288 10.1029/2005JD006987.
- 289 Cullen, D., J. Hubbell, and L. Kissel (1997), EPDL97: the evaluated photo data library97
290 version, *Tech. rep.*, UCRL-50400-Vol. 6-Rev. 5, Lawrence Livermore National Lab., CA
291 (United States).
- 292 Cummer, S. A., Y. Zhai, W. Hu, D. M. Smith, L. I. Lopez, and M. A. Stanley (2005),
293 Measurements and implications of the relationship between lightning and terrestrial
294 gamma ray flashes, *Geophys. Res. Lett.*, *32*, L08,811, doi:10.1029/2005GL022778.
- 295 Dwyer, J. R. (2005), The initiation of lightning by runaway air breakdown, *Geophys. Res.*
296 *Lett.*, *32*, L20,808, doi:10.1029/2005GL023975.
- 297 Dwyer, J. R. (2008), Source mechanisms of terrestrial gamma-ray flashes, *J. Geophys.*
298 *Res.*, *113*, D10,103, doi:10.1029/2007JD009248.

- 299 Dwyer, J. R., and D. M. Smith (2005), A comparison between Monte Carlo simulations of
300 runaway breakdown and terrestrial gamma-ray flash observations, *Geophys. Res. Lett.*,
301 *32*, L22,804, doi:10.1029/2005GL023848.
- 302 Dwyer, J. R., et al. (2004), A ground level gamma-ray burst observed in association with
303 rocket-triggered lightning, *Geophys. Res. Lett.*, *31*, 5119, doi:10.1029/2003GL018771.
- 304 Fargion, D. (2002), Discovering Ultra-High-Energy Neutrinos through Horizontal and Up-
305 ward τ Air Showers: Evidence in Terrestrial Gamma Flashes?, *Astrophys. J.*, *570*, 909–
306 925, doi:10.1086/339772.
- 307 Fishman, G. J., et al. (1994), Discovery of intense gamma-ray flashes of atmospheric
308 origin, *Science*, *264*(5163), 1313–1316.
- 309 Grefenstette, B., D. Smith, B. Hazelton, and L. Lopez (2009), First RHESSI terrestrial
310 gamma ray flash catalog, *J. Geophys. Res.*, *114*(A2).
- 311 Grefenstette, B. W., D. M. Smith, J. R. Dwyer, and G. J. Fishman (2008), Time
312 evolution of terrestrial gamma ray flashes, *Geophys. Res. Lett.*, *35*, L06,802, doi:
313 10.1029/2007GL032922.
- 314 Gurevich, A. V., K. P. Zybin, and R. A. Roussel-Dupré (1999), Lightning initiation by si-
315 multaneous effect of runaway breakdown and cosmic ray showers, *Phys. Lett. A*, *254*(1–
316 2), 79–87, doi:10.1016/S0375-9601(99)00091-2.
- 317 Hedin, A. E. (1991), Extension of the MSIS thermosphere model into the middle and
318 lower atmosphere, *J. Geophys. Res.*, *96*, 1159–1172, doi:10.1029/90JA02125.
- 319 Inan, U. S., and N. G. Lehtinen (2005), Production of terrestrial gamma-ray flashes by an
320 electromagnetic pulse from a lightning return stroke, *Geophys. Res. Lett.*, *32*, L19,818,
321 doi:10.1029/2005GL023702.

- 322 Inan, U. S., M. B. Cohen, R. Said, D. M. Smith, and L. I. Lopez (2006), Terrestrial
323 Gamma-ray Flashes and Lightning Discharges, *Geophys. Res. Lett.*, *33*, L18,802, doi:
324 doi:10.1029/2006GL027085.
- 325 Kossov, M. V. (2002), Approximation of photonuclear interaction cross-sections, *European*
326 *Physical Journal A*, *14*, 377–392.
- 327 Lehtinen, N. G., M. Walt, U. S. Inan, T. F. Bell, and V. P. Pasko (1996), γ -ray emission
328 produced by a relativistic beam of runaway electrons accelerated by quasi-electrostatic
329 thundercloud fields, *Geophys. Res. Lett.*, *23*(19), 2645–2648, doi:10.1029/96GL02573.
- 330 Lehtinen, N. G., T. F. Bell, and U. S. Inan (1999), Monte Carlo simulation of runaway
331 MeV electron breakdown with application to red sprites and terrestrial gamma ray
332 flashes, *J. Geophys. Res.*, *104*(A11), 24,699–24,712, doi:10.1029/1999JA900335.
- 333 Libby, L., and H. Lukens (1973), Production of radiocarbon in tree rings by lightning
334 bolts, *J. Geophys. Res.*, *78*, 5902–5903.
- 335 Marshall, T. C., M. Stolzenburg, C. R. Maggio, L. M. Coleman, P. R. Krehbiel, T. Hamlin,
336 R. J. Thomas, and W. Rison (2005), Observed electric fields associated with lightning
337 initiation, *Geophys. Res. Lett.*, *32*, 3813, doi:10.1029/2004GL021802.
- 338 Milikh, G., and J. A. Valdivia (1999), Model of gamma ray flashes due to fractal lightning,
339 *Geophys. Res. Lett.*, *26*(4), 525, doi:10.1029/1999GL900001.
- 340 Milikh, G. M., P. N. Guzdar, and A. S. Sharma (2005), Gamma ray flashes due to plasma
341 processes in the atmosphere: Role of whistler waves, *J. Geophys. Res.*, *110*(A9), 2308,
342 doi:10.1029/2004JA010681.
- 343 Paiva, G. S., A. C. Pavão, and C. C. Bastos (2009), “Seed” electrons from muon decay for
344 runaway mechanism in the terrestrial gamma ray flash production, *J. Geophys. Res.*,

- 345 114(D13), 3205, doi:10.1029/2008JD010468.
- 346 Roussel-Dupré, R. A., and A. V. Gurevich (1996), On runaway breakdown and upward
347 propagating discharges, *J. Geophys. Res.*, 101(A2), 2297–2312, doi:10.1029/95JA03278.
- 348 Shah, G. N., H. Razdan, Q. M. Ali, and C. L. Bhat (1985), Neutron generation in lightning
349 bolts, *Nature*, 313, 773–775, doi:10.1038/313773a0.
- 350 Shyam, A., and T. C. Kaushik (1999), Observation of neutron bursts associated with atmo-
351 spheric lightning discharge, *J. Geophys. Res.*, 104, 6867–6870, doi:10.1029/98JA02683.
- 352 Smith, D. M., L. I. Lopez, R. P. Lin, and C. P. Barrington-Leigh (2005), Terrestrial
353 gamma flashes observed up to 20 MeV, *Science*, 307(5712), 1085–1088, doi:10.1126/
354 science.1107466.
- 355 Stanley, M. A., X.-M. Shao, D. M. Smith, L. I. Lopez, M. B. Pongratz, J. D. Harlin,
356 M. Stock, and A. Regan (2006), A link between terrestrial gamma-ray flashes and
357 intracloud lightning discharges, *Geophys. Res. Lett.*, 33, L06,803.
- 358 Tierney, H. E., R. A. Roussel-Dupré, E. M. D. Symbalisty, and W. H. Beasley (2005),
359 Radio frequency emissions from a runaway electron avalanche model compared with
360 intense, transient signals from thunderstorms, *J. Geophys. Res.*, 110(D9), 12,109, doi:
361 10.1029/2004JD005381.

initial altitude	record type	initial direction distribution		
		up	down	isotropic
2.5 km	prod.	6468	6343	6436
	esc.	$< 1 (< 5 \times 10^{-3})$	$< 1 (< 5 \times 10^{-3})$	$< 1 (< 5 \times 10^{-3})$
	gnd.	1 (0.32)	229 (237)	23 (26.6)
5 km	prod.	6425	6485	6427
	esc.	$< 1 (0.13)$	$< 1 (< 5 \times 10^{-3})$	$< 1 (< 5 \times 10^{-3})$
	gnd.	$< 1 (< 5 \times 10^{-3})$	6 (6.5)	$< 1 (0.04)$
7.5 km	prod.	6434	6433	6343
	esc.	4 (4.7)	$< 1 (< 5 \times 10^{-3})$	2 (0.32)
	gnd.	$< 1 (< 5 \times 10^{-3})$	$< 1 (0.28)$	$< 1 (< 5 \times 10^{-3})$
10 km	prod.	6475	6420	6337
	esc.	34 (38.0)	$< 1 (0.03)$	3 (4.5)
	gnd.	$< 1 (< 5 \times 10^{-3})$	$< 1 (0.04)$	$< 1 (< 5 \times 10^{-3})$
15 km	prod.	5756	6323	6221
	esc.	452 (500)	15 (13.9)	113 (142)
	gnd.	$< 1 (< 5 \times 10^{-3})$	$< 1 (< 5 \times 10^{-3})$	$< 1 (< 5 \times 10^{-3})$
20 km	prod.	4250	6349	5923
	esc.	1107 (1238)	205 (228)	684 (794)
	gnd.	$< 1 (< 5 \times 10^{-3})$	$< 1 (< 5 \times 10^{-3})$	$< 1 (< 5 \times 10^{-3})$

Table 1. Neutrons produced and observed in simulations per million initial energetic photons. Numbers are for simulations of one million initial photons with a typical TGF energy spectrum but with energy $\mathcal{E}_\gamma > 9.87$ MeV, with < 1 indicating no neutrons were observed. Parenthetical numbers give the number of neutrons observed per million initial photons if the neutrons produced in the photon simulations are reproduced 200 times and allowed to propagate in the atmosphere to improve the statistics of propagation.

alt. (km)	gnd.	esc.
0.75	0.232	$< 3 \times 10^{-6}$
1	0.0916	$< 3 \times 10^{-6}$
1.25	0.0328	$< 3 \times 10^{-6}$
1.5	0.0116	$< 3 \times 10^{-6}$
1.75	4.2×10^{-3}	$< 3 \times 10^{-6}$
2	1.4×10^{-3}	$< 3 \times 10^{-6}$
2.25	4.2×10^{-4}	$< 3 \times 10^{-6}$
2.5	1.7×10^{-4}	$< 3 \times 10^{-6}$
2.75	7×10^{-5}	$< 3 \times 10^{-6}$
3	1.6×10^{-5}	$< 3 \times 10^{-6}$
3.25	1.1×10^{-5}	$< 3 \times 10^{-6}$
3.5	5×10^{-6}	$< 3 \times 10^{-6}$
5	$< 3 \times 10^{-6}$	$< 3 \times 10^{-6}$
7	$< 3 \times 10^{-6}$	$< 3 \times 10^{-6}$
10	$< 3 \times 10^{-6}$	$< 3 \times 10^{-6}$
12	$< 3 \times 10^{-6}$	5.0×10^{-4}
15	$< 3 \times 10^{-6}$	7.2×10^{-4}
17	$< 3 \times 10^{-6}$	0.0396
20	$< 3 \times 10^{-6}$	0.111
25	$< 3 \times 10^{-6}$	0.318

Table 2. Number of neutrons that reach ground and satellite altitude per neutron injected in an isotropic point source at the indicated altitude with the characteristic energy spectrum shown in Figure 1.

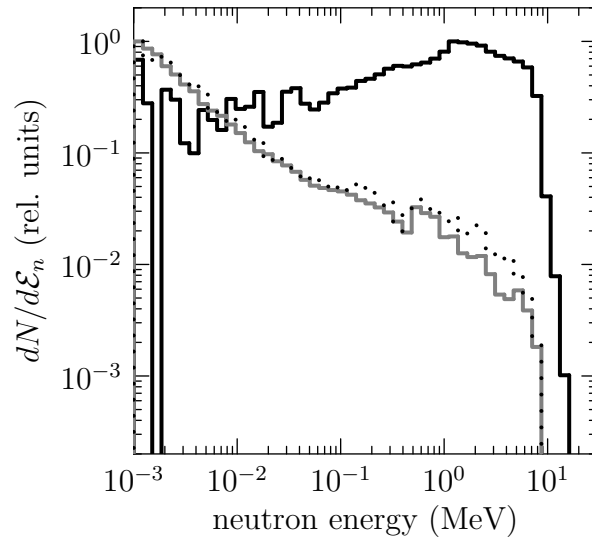


Figure 1. Characteristic energy spectrum of neutrons when produced (solid black curve). Also shown are the spectrum of neutrons reaching ground from downward-directed source at 2.5 km (black dotted) and satellite altitude from upward-directed source at 20 km (grey solid).

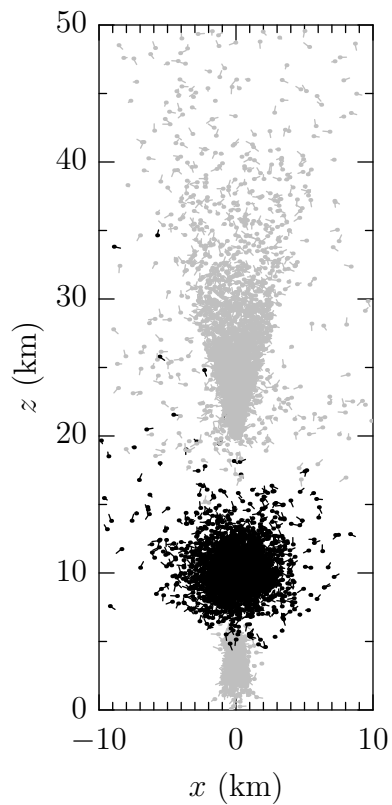


Figure 2. Position and direction of motion of neutrons when produced. Each dot represents the production a neutron, with the line segment extending outward in the direction of motion of the neutron. Upper gray cluster: 20 km initial altitude, upward-directed 20° beam. Central black cluster: 10 km initial altitude, isotropic. Lower grey cluster: 5 km initial altitude, downward-directed 20° beam.

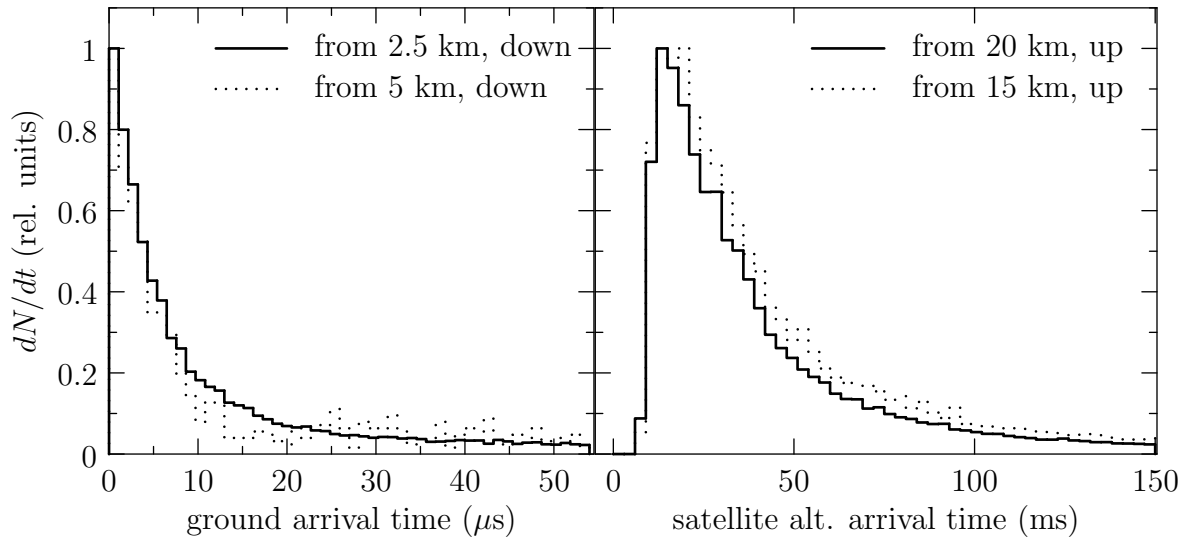


Figure 3. Neutron arrival time distributions. Left: neutrons arriving at ground level from a downward-directed photon source at 2.5 km altitude, right: neutrons arriving at 350 km altitude from an upward-directed photon source at 20 km altitude. Note the different timescales. The long timescale in the right panel is due to longer scattering path lengths, not merely longer path lengths from source to satellite plane.

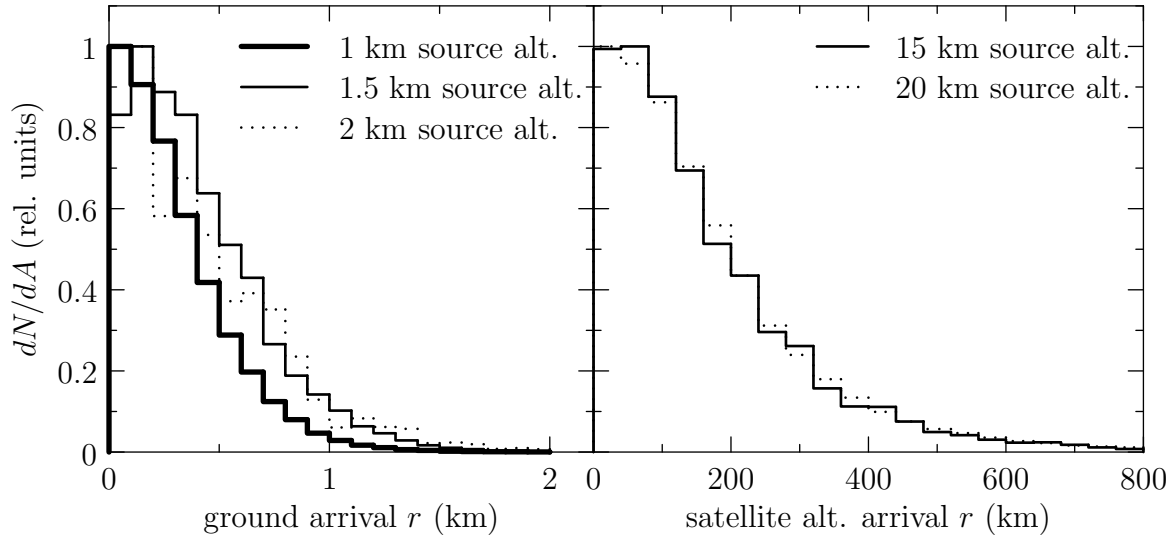


Figure 4. Number of neutrons per unit area vs. radial distance from the sub-source point for neutrons produced in a point source at the altitude indicated on the plot. Ground level (left), 350 km altitude (right).